Altered Glia-Neuron Communication in Alzheimer's Disease Affects WNT, p53, and NFkB Signaling Determined by snRNA-seq

Tabea M. Soelter[1], Timothy C. Howton[1], Amanda D. Clark[1], Vishal H. Oza[1], Brittany N. Lasseigne*[1]

Affiliations:

1. Department of Cell, Developmental and Integrative Biology, Heersink School of Medicine, The University of Alabama at Birmingham, Birmingham, Alabama, United States of America

Co-author email addresses:

Tabea M. Soelter: tsoelter@uab.edu, Timothy C. Howton: tchowton@uab.edu, Amanda D. Clark: clarkad@uab.edu, Vishal H. Oza: vishoza@uab.edu, Brittany N. Lasseigne: bnp0001@uab.edu
(*corresponding author)

Abstract

Background:

Alzheimer's disease is the most common cause of dementia and is characterized by amyloid-β plaques, tau neurofibrillary tangles, and neuronal loss. Although neuronal loss is a primary hallmark of Alzheimer's disease, it is known that non-neuronal cell populations are ultimately responsible for maintaining brain homeostasis and neuronal health through neuron-glia and glial cell crosstalk. Many signaling pathways have been proposed to be dysregulated in Alzheimer's disease, including WNT, TGFβ, p53, mTOR, NFkB, and Pi3k/Akt signaling. Here, we predict altered cell-cell communication between glia and neurons.

Methods:

Using public snRNA-sequencing data generated from postmortem human prefrontal cortex, we predicted altered cell-cell communication between glia (astrocytes, microglia, oligodendrocytes, and oligodendrocyte progenitor cells) and neurons (excitatory and inhibitory). We confirmed interactions in an independent orthogonal dataset. We determined cell-type-specificity using Jaccard Similarity Index and investigated the downstream effects of altered interactions in inhibitory neurons through gene expression and transcription factor activity analyses of signaling mediators. Finally, we determined changes in pathway activity in inhibitory neurons.

Results:

Cell-cell communication between glia and neurons is altered in Alzheimer's disease in a cell-type-specific manner. As expected, ligands are more cell-type-specific than receptors and targets. We validated 51 ligand-receptor pairs in an independent dataset that included two known Alzheimer's disease risk genes: *APP* and *APOE*. 17 (14 upregulated and 3 downregulated in Alzheimer's disease) of the 51 interactions also had the same downstream target gene. Most of the signaling mediators of these interactions were not differentially expressed, however, the mediators that are also transcription factors had differential activity between AD and control. Namely, *MYC* and *TP53*, which are associated with WNT and p53 signaling, respectively, had repressor activity in Alzheimer's disease, along with decreased WNT and p53 activity in inhibitory neurons. Additionally, inhibitory neurons had both increased NFkB signaling pathway activity and activator activity of *NFIL3*, an NFkB signaling-associated transcription factor.

Conclusions:

Cell-cell communication between glia and neurons in Alzheimer's disease is altered in a cell-type-specific manner involving Alzheimer's disease risk genes. Signaling mediators had altered transcription factor activity suggesting altered glia-neuron interactions may dysregulate signaling pathways including WNT, p53, and NFkB in inhibitory neurons.

Keywords
Alzheimer's disease, neurodegeneration, cell-cell communication, signaling, single-cell, networks, genomics

Background

Alzheimer's disease (AD) is the most common cause of dementia, and an estimated 55 million people have dementia worldwide [1]. AD is characterized by amyloid-β plaques and phosphorylated tau tangles that result in neuronal loss, leading to memory deficits and overall cognitive decline [2]. While there are identified causes of familial early-onset AD, the causes of sporadic late-onset AD are largely unknown. Although neuronal loss is a primary hallmark of AD, it is known that non-neuronal cell populations maintain brain homeostasis and neuronal health through neuron-glia and glial cell crosstalk via chemical messengers [3–6]. For example, astrocytes provide metabolic and nutritional support to neurons, while oligodendrocytes are responsible for neuron axon myelination [7–9]. Additionally, oligodendrocyte progenitor cells (OPCs) are in direct contact with neuronal synapses, and signaling between OPCs and other cell types, including glia and endothelial cells, has been previously indicated [10]. Microglia, as the resident macrophages of the central nervous system (CNS), release cytokines, chemokines, and growth factors in response to injury, which influence the synaptic activity of neurons [11–13]. Yet the glia-neuron interactions altered in AD have not been fully investigated despite being critical for understanding disease mechanisms and their potential as targets for therapeutic intervention. Between 2003 and 2021, no AD-mitigating therapeutics were approved by the FDA [14]. Aducanumab and lecanemab were approved in 2021 and 2023, respectively, despite concerns about their safety and efficacy, underscoring that the need for novel therapeutic targets persists.

Multiple signaling pathways have been proposed to be dysregulated in AD, including WNT (reviewed in [15, 16]), TGFβ (reviewed in [17–19]), mTOR (reviewed in [20, 21]), NFkB (reviewed in [22, 23]), p53 (reviewed in [24]), and Pi3k/Akt signaling (reviewed in [25–27]). Recently, multiple computational cell-cell communication (CCC) inference tools, which use single-nucleus RNA-sequencing (snRNA-seq) data to infer ligands and receptors, were developed to predict signaling patterns between cell types (reviewed in [28]). Using these approaches, CCC patterns in the human postmortem prefrontal cortex (PFC) were previously shown to be disrupted in AD compared to control patients [29, 30]. For example, chandelier neurons were associated with an inhibitory signaling pattern in control PFC, though in AD they were associated with excitatory signaling involved in the WNT signaling pathway [29]. Additionally, signaling involving glial cells, such as astrocytes and microglia, had an increased involvement of known AD-risk and neuroinflammatory genes in predicted ligands and receptors [29, 30]. While previous studies investigated overall patterns of altered CCC across all cell types without specifically describing altered glia-neuron interactions or focused on interactions between neurons and microglia [29–31], altered glia-neuron interactions and their downstream consequences in neurons remain understudied in AD.

Here, we used publicly available snRNA-seq AD and control (CTRL) data generated from postmortem human PFC to study altered glia-neuron interactions and their downstream effects in AD (**Fig 1A**) [32]. We inferred differential CCC interactions between astrocytes, microglia, oligodendrocytes, or OPCs (sender cell types) and inhibitory or excitatory neurons (receiver cell types; **Fig 1B**). We also investigated whether CCC is similar across cell types by calculating the Jaccard Similarity Index (JI) of ligands, receptors, and target genes between cell types (**Fig 1C**). We also validated our interactions using an independent human PFC AD snRNA-seq dataset [33] and further investigated the resulting high-confidence ligand-receptor pairs from both data sets, their predicted downstream target genes, and signaling modulators through transcription factor (TF) and canonical signaling pathway activity (**Fig 1D-E**).

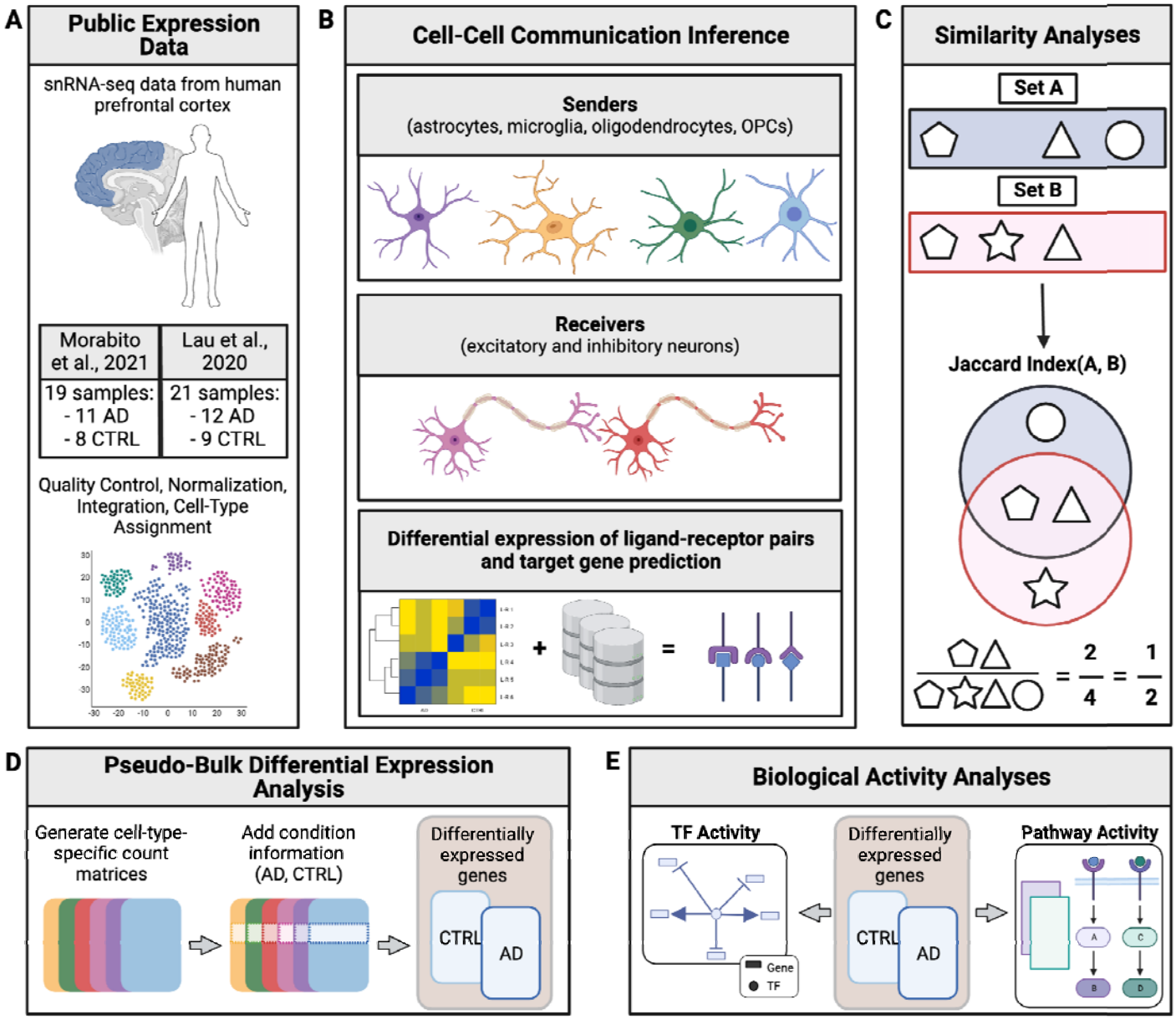

Figure 1. Schematic overview of our study design. (A) We downloaded and processed two publicly available snRNA-seq datasets from human postmortem prefrontal cortex (PFC) with Alzheimer's disease (AD) as well as age- and sex-matched controls. **(B)** We inferred ligand-receptor pairs between senders (astrocytes, microglia, oligodendrocytes, and oligodendrocyte progenitor cells - OPCs) and receivers (excitatory and inhibitory neurons) using gene expression and known ligand-receptor information. We also predicted target genes downstream of the ligand-receptor pairs [34]. **(C)** To determine whether interactions were cell-type-specific or shared, we calculated the Jaccard Similarity Index (JI) of ligands, receptors, and targets in senders and receivers. Shapes can refer to either ligands, receptors, or targets. **(D)** Then, we generated cell-type-specific count matrices to determine differentially expressed genes. **(E)** Using the differentially expressed genes, we inferred transcription factor (TF) activity of signaling mediators that are TFs and investigated canonical pathway activity [35].

Methods

Data Acquisition and Alignment

We downloaded 2 publicly available snRNA-seq datasets (GSE174367 [32], GSE157827 [33]) generated from postmortem human PFC using the SRA-Toolkit v3.0.0. Both datasets include AD as well as age- and sex-

matched control samples (GSE174367: 11 AD and 8 control, GSE157827: 12 AD and 9 control). We aligned FASTQ files to the 10x Genomics human reference genome (GRCh38) on the UAB Cheaha supercomputer using 10x Genomics Cell Ranger 6.1.1 [36].

Data Processing and Quality Control

We performed all analyses in docker [37] with R v4.1.3 (**Availability of data and materials)**. Since GSE157827 had increased levels of ambient RNA after alignment, we performed ambient RNA removal using SoupX [38] v1.6.2 on Cell Ranger h5 files, which resulted in filtered Cell Ranger output matrices. We did not remove ambient RNA from GSE174367, as there was no evidence of increased ambient RNA levels. We used version 4.3.0.9002 of the Seurat R package for our analyses [39]. We combined Cell Ranger output matrices into sparse expression matrices using the *Read10x* function [39]. We created a Seurat object using the *CreateSeuratObject* function for each sample and condition (AD and control) before merging them into a single Seurat object. We performed quality control metrics at both the cell (i.e., mitochondrial ratio < 0.2, log10 of the number of genes per UMI > 0.8, and the number of genes per cell) and gene level (i.e., removing zero count values to prevent skewing of average expression values, therefore retaining genes expressed in 10 cells or more). We filtered GSE174367 and included cells with > 1,000 and < 10,000 genes per cell and we filtered GSE157827 to include cells with > 500 and < 10,000 genes per cell. Then, using default parameters, we performed batch correction within each dataset using harmony v0.1.0 [40], as it preserves biological variation while reducing variation due to technical noise [41]. We also performed Principal Component Analysis (PCA) using the *RunPCA* function from Seurat [39] without approximation (approx = FALSE). We scaled and normalized features/genes before plotting UMAPs to confirm successful integration across conditions.

Clustering and Cell Type Identification

In order to determine clustering resolution, we compared multiple resolutions between 0 and 2 using clustree v0.5.0 for each dataset [42]. We chose resolutions 1.2 and 1, which identified 32, and 34 clusters using leiden v0.4.3 [43] for GSE174367 and GSE157827, respectively. We identified differentially expressed marker genes for each cluster (using the *FindAllMarkers* function on the RNA assay from Seurat [39]) with a log fold change threshold > 0.2 and a significant Bonferroni adjusted p-value. We assigned cell types using differential expression of cell-type-specific genes (**Tables S1 and S2**) identified through PanglaoDB [44], CellMarker [45], and the Human Protein Atlas [46] at https://www.proteinatlas.org/ and feature plots using canonical cell type markers (**Table S3**). We sub-clustered neuron clusters initially unidentifiable as excitatory or inhibitory using the *FindSubCluster* function from Seurat [39] and assigned their cell type through differential expression (log fold change threshold > 0.25) of marker genes.

Cell-Cell Communication Inference

To infer CCC between glia and neurons across conditions (AD and CTRL), we applied multinichenetr v1.0.0 and used the Nichenet v2 prior [34]. We converted our processed Seurat objects to Single Cell Experiment objects using the SingleCellExperiment R package [47] v1.16.0 before using them as input to MultiNicheNet. Then, we performed ligand-receptor pair prediction between all cell types in each dataset and filtered for senders (astrocytes, microglia, oligodendrocytes, and OPCs) and receivers (excitatory and inhibitory neurons) between conditions. Since MultiNicheNet uses pseudobulk aggregation for its differential expression analysis, we only included samples with a minimum of 10 cells per cell type per sample. We identified differentially expressed ligands, receptors, and target genes using a 0.5 logFC threshold with non-adjusted p-values of 0.05, as recommended by the package developers. When calculating ligand activity, we considered the top 250 targets with the highest regulatory potential. We prioritized ligand-receptor interactions by min-max scaling the scores for all comparisons of the following metrics: differential expression of ligand, differential expression of the receptor, the fraction of ligand-receptor pairs expressed across samples, expression of ligand, expression of the receptor, scaled ligand activity, the abundance of the sender in the condition of interest, and

abundance of the receiver in the condition of interest. Then, we performed weighted aggregation of the scaled scores using default MultiNicheNet prioritization weights. We calculated expression correlation information between ligand-receptor pairs and their targets by calculating Pearson and Spearman correlation coefficients. Downstream analyses only included ligand-receptor-target (LRT) interactions with Spearman and Pearson correlation coefficients greater than 0.33 and less than -0.33, as recommended. Finally, we compiled a list of high-confidence LRTs. High-confidence interactions were LRTs that met previous filtering criteria in both datasets while involving the same sender and receiver cell type.

Similarity Calculations of Ligands, Receptors, and Target Genes Across Cell Types

We calculated the JI to determine the degree of overlap of ligands, receptors, and target genes between sender or receiver cell types. First, we calculated JI between receiver cell types (excitatory and inhibitory neurons) based on the overlap of receptors and target genes. Then, we calculated JI between sender cell types (astrocytes, microglia, oligodendrocytes, and OPCs) based on the overlap of ligands, receptors, and target genes.

Gene Regulatory Network Inference

For every high-confidence LRT, we generated gene regulatory networks (active signaling networks) that included the top 2 regulators (based on whether they were upstream of the target and downstream of the ligand) in each dataset with the *get_ligand_signaling_path_with_receptor* function from multinichenetr v1.0.0 R package [34]. We scored and ranked signaling regulators based on whether they were upstream of the target gene and downstream of the ligand. We assigned edge weights to the networks by combining them with MultiNicheNet's prior knowledge, which includes information on ligand-receptor to target signaling paths. Then, we investigated the active signaling networks' topology using the igraph v1.5.1 R package [48]. We generated weighted and directed igraph objects for individual LRT-specific active signaling networks using the *graph_from_data_frame* function. Then, we determined all potential signaling mediators by identifying nodes outgoing from the receptor node using the *neighbors* function. Finally, we determined the shortest path between the receptor and target gene nodes using the *shortest_paths* function using Dijkstra's algorithm to infer the most likely path and, therefore, the top mediator(s) of signal transduction of our high-confidence interactions (**Table 1**).

Pseudo-bulking of snRNA-seq Data

To overcome the data sparsity in snRNA-seq [49], we pseudo-bulked both of our datasets and generated cell-type-specific count matrices, as previously described [50]. We converted raw data from the Seurat object *counts* slot into Single Cell Experiment objects using SingleCellExperiment [47] v1.16.0 while also incorporating necessary metadata with information on sample origin (sample_id), condition (group_id), and cell type (cluster_id). We aggregated counts for each cell type across samples using the *aggregate.Matrix* function (Matrix.utils R package v0.9.7), yielding gene by sample counts for each cell type. We appended the metadata with condition information (AD or CTRL) in preparation for our differential gene expression analysis (see below).

Differential Gene Expression Analysis

We performed differential gene expression analysis between conditions (AD vs CTRL) using DESeq2 v1.34.0 for each cell type [51]. First, we created dds objects using the *DESeqDataSetFromMatrix* function. We made pairwise comparisons for every cell type between conditions using the Wald test. Then, we performed log fold change shrinkage to generate more accurate log2foldchange estimates. While DESeq2 recommends the application of Bayesian log fold change shrinkage (type = apeglm), we used its original shrinkage estimator (type = normal), as it preserves the Wald test statistic (*stat*) needed for our downstream analyses of TF and pathway activity.

Transcription Factor Activity Analysis

To determine whether transcription factors (TFs) that are signaling mediators had activator or repressor roles in inhibitory neurons, we used the Wald test statistic (*stat*) from previously generated pseudo-bulk differential gene expression analysis outputs. To compare across both datasets, we combined *stat* scores from both datasets into one data frame before inferring TF activity. However, as datasets did not have the same number of identified differentially expressed genes, we replaced NAs with 0. We used the CollecTRI prior (accessed in September 2023), which has information on TFs, including their direction of regulation on their targets [52], and combined it with pseudo-bulked count matrices for inhibitory neurons. We calculated activity scores for all TFs in inhibitory neurons that had a minimum of 5 targets using the Multivariate Linear Model (*run_mlm* function decoupleR v2.7.1 [35]), where the t-values from the model represent regulator activity [35]. Positive values represent an activator role, while negative values represent a repressor role in AD compared to control. After inferring TF activity, we subsetted for TFs that were signaling mediators in our high-confidence LRTs in inhibitory neurons.

Pathway Activity Analyses

Similarly to our TF activity analysis, we used the Wald test statistic (*stat*) from pseudo-bulk differential gene expression analysis outputs to infer pathway activity in inhibitory neurons. As before, we replaced NAs with 0, as the datasets did not have the same number of differentially expressed genes. We used the top 500 responsive genes ranked by p-value in PROGENy, a collection of pathways and their target genes (accessed in October 2023) [53]. We calculated pathway activity scores for all pathways with a minimum of 5 targets using the Multivariate Linear Model (*run_mlm* function decoupleR v2.7.1 [35]). Positive values represent an increase, while negative values represent a decrease in pathway activity in AD compared to CTRL.

Results

Identification of cell-cell communication patterns from AD snRNA-seq data

To infer cell-cell communication (CCC) patterns in AD, we used previously published snRNA-seq data generated from 19 postmortem human PFC, including 11 AD and 8 age- and sex-matched CTRL samples (Morabito et al., 2021, **Fig 2**) [32]. We aligned raw fastq files and retained ~65K nuclei after quality control. We identified 32 distinct clusters using Leiden clustering [43], and assigned eight major brain cell types using differential expression of canonical marker genes (**Fig 2A-B, Tables S1-3**). Cell types were evenly distributed and integrated across conditions (AD, CTRL, **Fig. 2C**). Next, we determined whether cell types were balanced across conditions. We observed that all cell type proportions were slightly biased towards AD (**Fig 2D).** However, as there is an imbalance of AD to control samples in the dataset (11 and 8, respectively), we expected this.

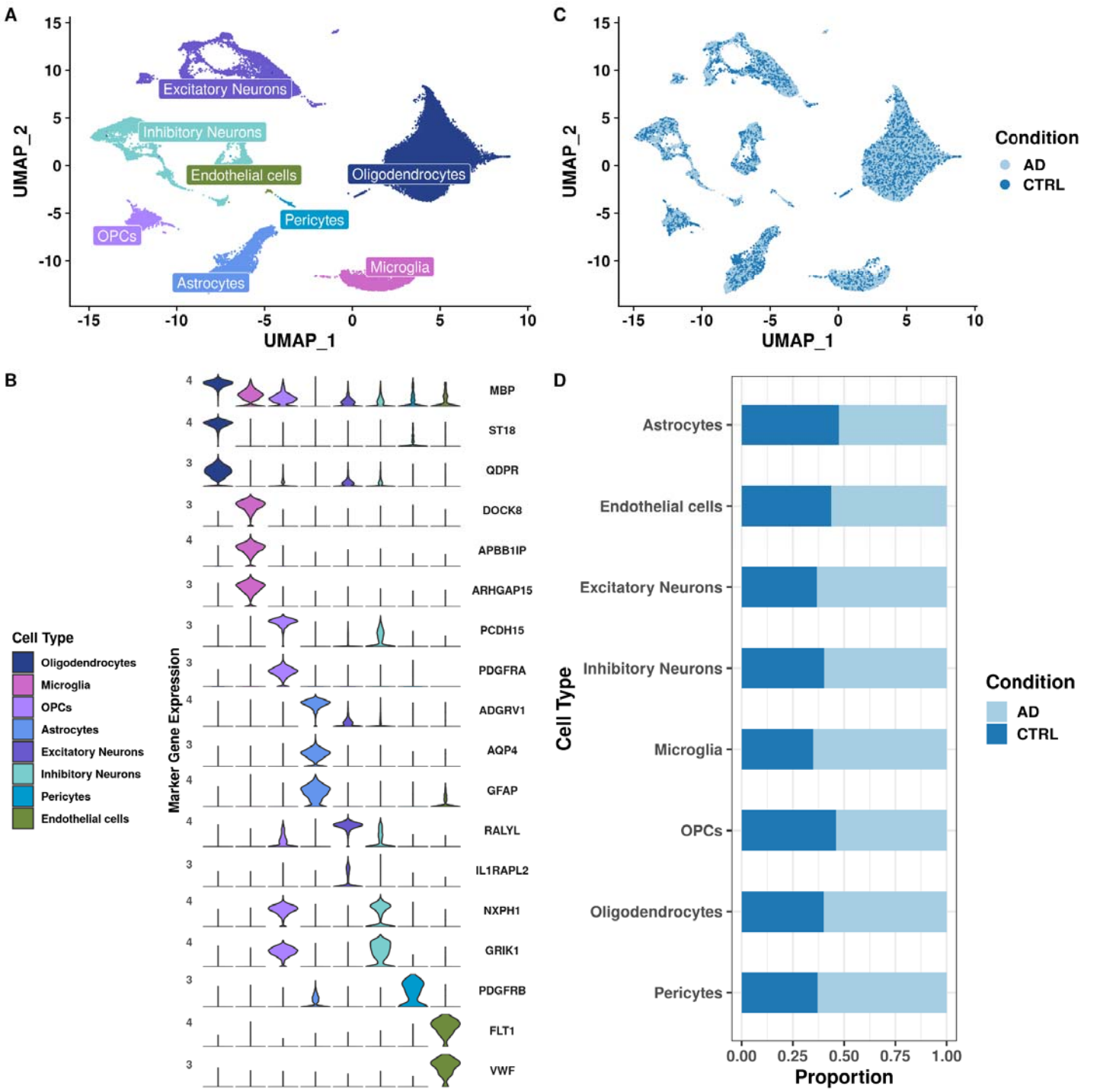

Figure 2. Overview of our approach and dataset (A) Uniform Manifold Approximation and Projection (UMAP) of 65,546 nuclei colored by their assigned cell types. **(B)** Violin plot of canonical marker gene expression used for cell type assignment. Color represents cell type. **(C)** UMAP of integrated dataset split by condition (AD, CTRL). **(D)** Stacked barplot of cell type proportions across conditions (AD, CTRL).

Ligand, receptor, and target gene patterns are mostly cell-type-specific in AD

We predicted interactions using MultiNicheNet [34] by determining genes differentially expressed between AD and CTRL in all cell types before filtering for our sender (astrocytes, microglia, oligodendrocytes, and OPCs) and receiver (excitatory and inhibitory neurons) cells of interest (**Fig 1B**). By cross-referencing differentially expressed genes with the NicheNet prior, we identified more than 45,000 differentially expressed ligand-receptor interactions between AD and control across all cell types (**Fig S2A**). After filtering interactions based

on our senders and receivers of interest (**Fig S2B**) and prioritizing interactions based on ligand activity and regulatory potential [34], we were left with 1,618 ligand-receptor-target (LRT) pairings (**Fig 3A**)**.** 1,334 of the 1,618 predicted interactions were up-regulated in AD, and 284 were up-regulated in CTRL, suggesting their decreased expression and, therefore a loss of signal in AD (**Fig S2C**). Most interactions originated from OPCs (n = 647), followed by astrocytes (n = 355), microglia (n = 316), and oligodendrocytes (n = 300). Interestingly, OPCs had the fewest (n = 3,097), and oligodendrocytes had the most nuclei (n = 38,864). In contrast, astrocytes and microglia had 5,272 and 3,862 nuclei, respectively, suggesting that the number of predicted interactions is independent of the number of nuclei in each cell type. Of the 1,618 prioritized LRTs, 778 were specific to excitatory, and 840 were specific to inhibitory neurons (**Fig 3A**). To determine whether CCC patterns were cell-type-specific or shared, we compared ligands, receptors, and target genes by Jaccard Similarity Index (JI). JI scores range from 0 (no overlap, i.e., cell-type specific) to 1 (total overlap, i.e., shared). In order to determine the similarity between excitatory and inhibitory neuron signaling patterns, we calculated their JI with respect to senders for receptor and target genes only. Since ligands are specific to senders and not receivers, we did not evaluate their overlap in excitatory and inhibitory neurons. Overall, receptors and target genes were not highly similar between neuronal subtypes (JI < 0.5 for all comparisons; **Fig 3B**). Interestingly, we observed overall higher JI in receptors (JI 0.13 - 0.44) than in target genes (JI 0.1 - 0.18), indicating differential downstream effects despite overlapping receptors between excitatory and inhibitory neurons (**Fig 3B**). In addition to comparisons between receiver cell types, we were interested in the similarity of ligands, receptors, and target genes between sender cell types by neuron subtypes (**Fig 3C-H**). For ligands associated with inhibitory neurons, the greatest overlap was between ligands from OPCs and astrocytes (JI = 0.12), closely followed by oligodendrocyte-OPC (JI = 0.1) interactions (**Fig 3C**). For ligands interacting with excitatory neurons, OPCs and oligodendrocytes had the highest similarity with astrocytes (JI = 0.14 for both; all other comparisons JI < 0.11; **Fig 3F**). Additionally, microglia-expressed ligands had the lowest similarity to all other sender cell types in both receivers (**Fig 3C & Fig 3F**). Receptor JI scores were higher overall than ligands, and OPCs had the highest similarity score with astrocytes for both receiver cell types (inhibitory JI = 0.25, **Fig 3D** and excitatory JI = 0.21, **Fig 3G**). Finally, the target genes of inhibitory and excitatory neurons had a higher JI than ligands or receptors (**Fig 3E & 3H**). The greatest overlap of target genes in inhibitory neurons was between microglia and astrocytes (JI = 0.46; **Fig 3E**), despite microglia- and astrocyte-expressed ligands having low similarity (JI = 0.05; **Fig 3C**). Within inhibitory neurons, OPCs and oligodendrocytes shared the least number of target genes (JI = 0.32; **Fig 3E**). We observed the same pattern of high target gene similarity with low ligand similarity between senders in excitatory neurons (e.g., microglia-astrocytes: target JI = 0.28 and ligand JI = 0, **Fig 3F and 3H**). Overall, OPCs and astrocytes showed similar and consistent overlap across ligands, receptors, and targets with both inhibitory and excitatory neurons (**Fig 3C-H**). We performed the same analyses in an independent snRNA-seq dataset (Lau et al., 2020) [33] from the same brain region. The Lau et al. dataset included 21 human postmortem PFC samples (12 AD, 9 control). As with the Morabito et al. data, we aligned fastq files and assigned cell types using differential expression of canonical marker genes (**Fig S1A-B**). We integrated ~32,000 cells across conditions (**Fig S1C**), which resulted in 7 cell types (**Fig S1A**). Finally, the cell type proportions were balanced across conditions for all but the endothelial cells, which had an increased proportion in AD (75% AD, 25% CTRL; **Fig S1D**). After differential CCC analysis, we identified fewer total interactions (n = 887) in the Lau et al. data, and as before in Morabito et al., we predicted more interactions specific to inhibitory neurons (n = 543) compared to excitatory neurons (n = 344; **Fig S3A**). Similarly, receptors and target genes were not highly similar between neuronal subtypes (JI < 0.2 for all comparisons, **Fig S3B**), and target genes between senders had a higher JI than ligands and receptors in both excitatory and inhibitory neurons in the validation dataset (**Fig S3C-H**). Generally, the results from our independent validation dataset recapitulate our original findings. Overall, we found that ligands, receptors, and target genes are largely cell-type-specific between and across sender and receiver cell types in two datasets. This supports cell-type-specific altered CCC patterns in AD.

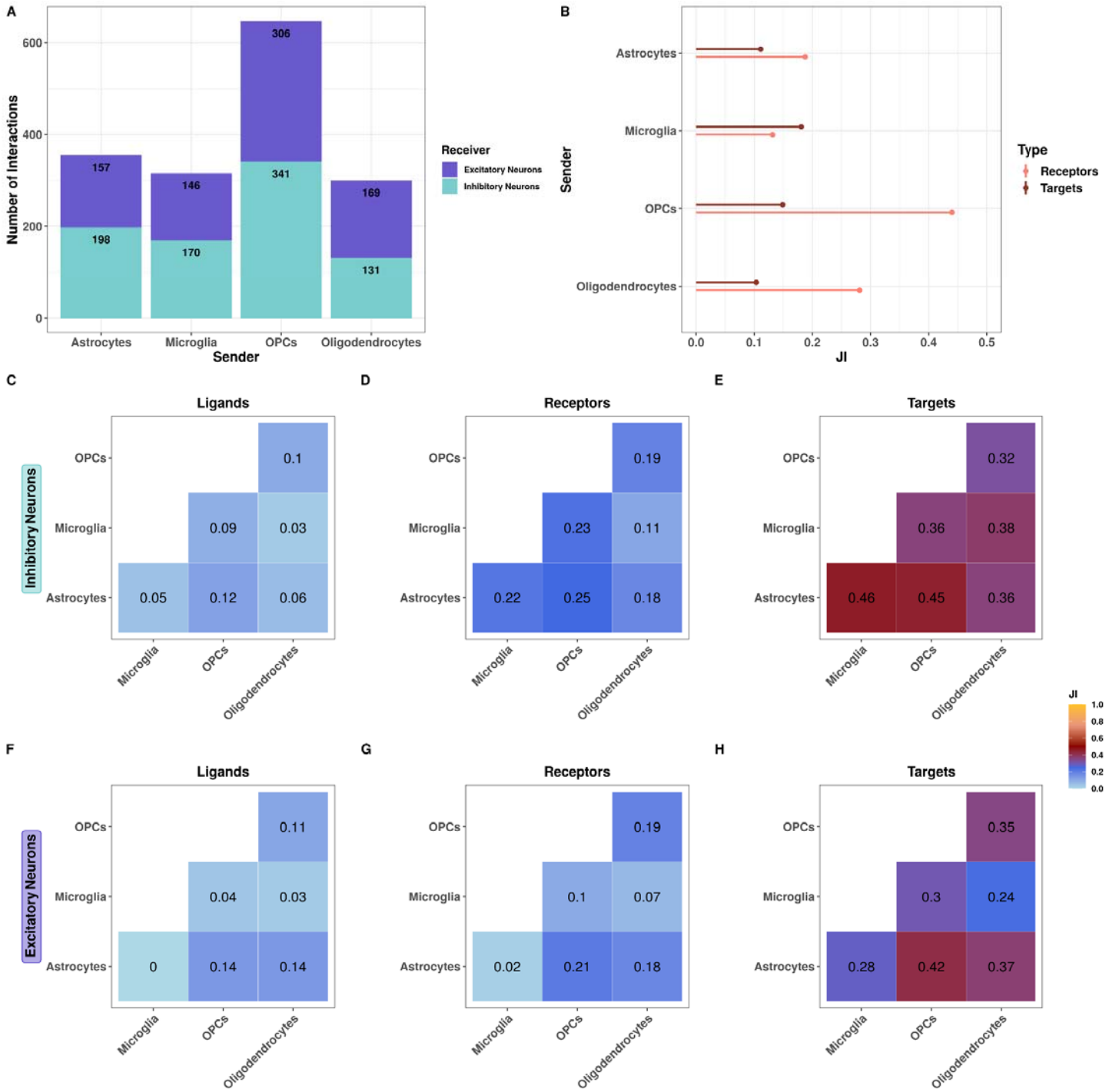

Figure 3. Ligand, receptor, and gene target patterns are mostly cell-type-specific in AD (A) Stacked barplot of the number of prioritized interactions where excitatory or inhibitory neurons are the receiver. **(B)** Jaccard Similarity Index (JI) between excitatory and inhibitory neurons of receptors and targets. JI between sender cell type **(C)** ligands, **(D)** receptors, and **(E)** targets for inhibitory neurons**.** JI between sender cell type **(F)** ligands, **(G)** receptors, **(H)** targets for excitatory neurons.

<u>Analyses of altered CCC in 2 datasets reveal shared ligands-receptor pairs and downstream target genes</u>

To determine high-confidence interactions that were conserved across multiple AD patient cohorts, we determined the overlap of altered CCC interactions (both ligand-receptor and LRTs) identified in both datasets. We identified 43 ligand-receptor pairs that were upregulated in AD with the same sender and receiver cell type

across datasets, comprised of 29 ligands and receptors (**Fig S4A**). Out of 29 ligands, only CADM2 and NRG2 were predicted in more than 1 cell type, while multiple ligands from more than one sender cell type jointly targeted 7 receptors (CADM3, ACVR2A, APP, ACVR1B, EGFR, LRRTM2, PLXNA; **Fig S4**). Additionally, we identified 8 ligand-receptor pairs that were upregulated in CTRL, which we inferred as interactions lost or downregulated in AD. Interestingly, these interactions included 2 AD-risk genes as ligands: APP and APOE, predicted in oligodendrocytes and astrocytes, respectively (**Fig S4B**). Except for OPCs, we find that ligand-receptor pairs overlapping across datasets seem to be receiver-specific, as no interactions are shared between excitatory and inhibitory neurons (**Fig 4A**). Additionally, oligodendrocytes were the only sender across both datasets that had overlapping communication with excitatory neurons only (**Fig 4A**). We also predicted APP as a receptor in both excitatory and inhibitory neurons through ligands from OPCs and microglia, respectively (**Fig 4A**). Additionally, we also identified APP as a ligand in oligodendrocytes interacting with GPC1 in excitatory neurons, while the risk factor APOE functions as a ligand in astrocytes interacting with LRP8 in inhibitory neurons (**Fig 4A**). Both of these interactions were downregulated in AD. We identified EGFR as an inhibitory neuron receptor in 3 of 4 senders (oligodendrocytes had no overlapping interactions with inhibitory neurons; **Fig 4A**), which has been proposed as a therapeutic target in AD [54, 55]. However, ligands targeting EGFR were dependent on the sender cell type. Out of 51 ligand-receptor pairs identified in both datasets, only 17 also shared the same downstream target gene (**Fig 4B**). In comparison, the 34 remaining ligand-receptor pairs did not show target gene overlap (**Table S4**). Our 17 high-confidence LRTs included interactions originating from all senders and converged to four target genes: *SMAD7*, *LMO1*, *PRLR*, and *CCND1* (**Fig 4B**). Interestingly, most of our high-confidence interactions originated from OPCs (n = 8) and astrocytes (n = 7). The interactions involving the AD-risk genes *APP* and *APOE,* as well as *EGFR,* also remained among our high-confidence interactions. Additionally, pseudo-bulk expression information for the four overlapping target genes confirms the same gene expression directionality across datasets in AD, where *LMO1* and *PRLR* were upregulated in excitatory neurons, while *SMAD7* and *CCND1* are up- and downregulated, respectively, in inhibitory neurons across datasets (**Fig 4C**). Altogether, we showed that ligand-receptor pairs are mostly receiver-specific and that the majority of our senders, except for oligodendrocytes, had altered CCC with both excitatory and inhibitory neurons across AD datasets. Our findings also indicate that interactions involving AD-risk or AD-associated genes (like *EGFR*) are preserved across different patient cohorts.

Figure 4. Ligand-receptor pairs and target genes overlap between 2 independent snRNA-seq datasets from the same brain region (A) Alluvial plots of overlapping ligand-receptor pairs for each sender cell type colored by receiver cell type. **(B)** Alluvial plot of the 17 ligand-receptor-target pairings that overlap across datasets, colored by sender cell type. Grey indicates the involvement of more than one sender cell type. **(C)** Heatmap of pseudo-bulk expression values for target genes which were identified in both datasets annotated by receiver cell type and dataset.

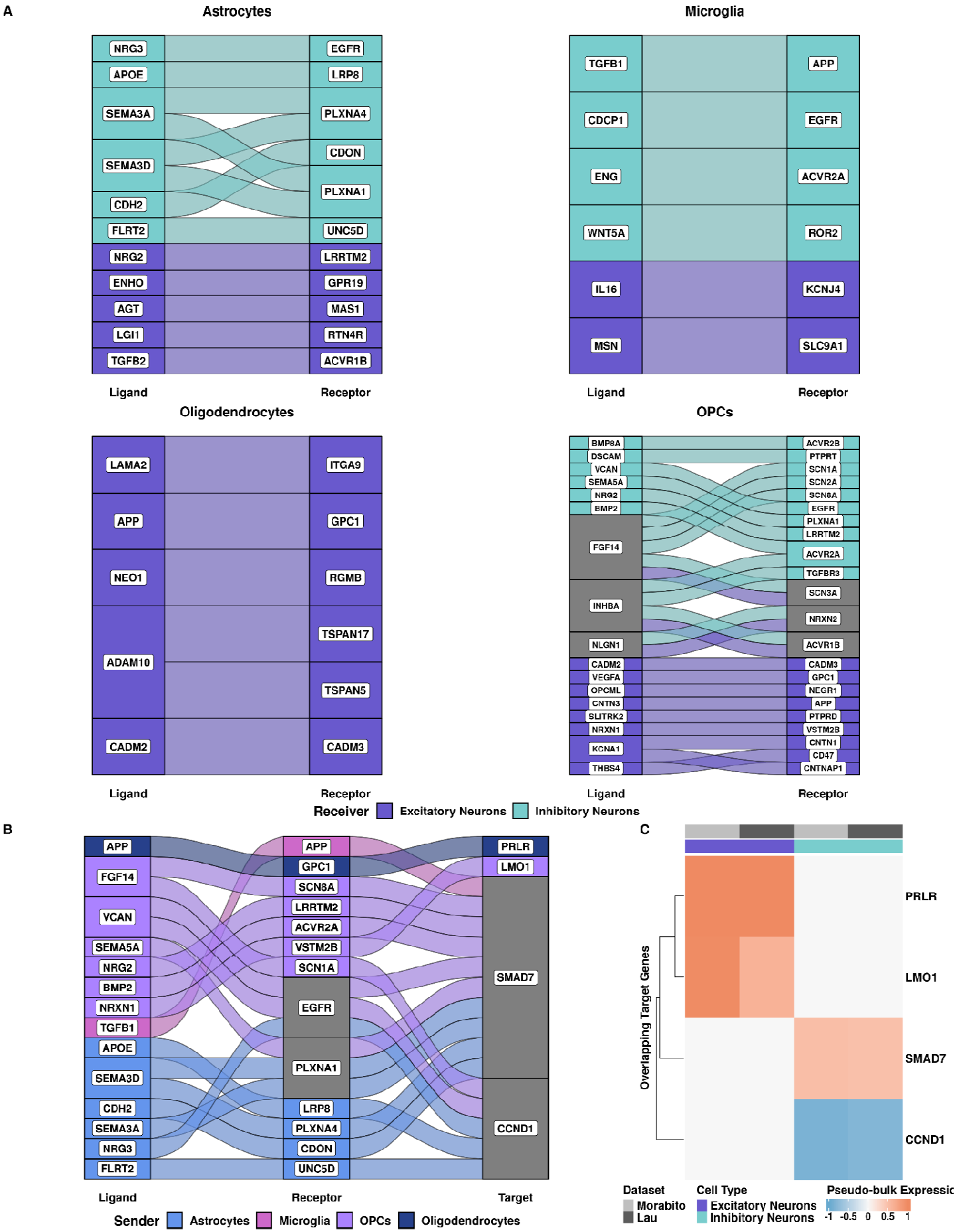
A
Astrocytes
NRG3
APOE
SEMA3A
SEMA3D
CDH2
FLRT2
NRG2
ENHO
AGT
LGI1
TGFB2
EGFR
LRP8
PLXNA4
CDON
PLXNA1
UNC5D
LRRTM2
GPR19
MAS1
RTN4R
ACVR1B
Ligand
Receptor
Microglia
TGFB1
CDCP1
ENG
WNT5A
IL16
MSN
APP
EGFR
ACVR2A
ROR2
KCNJ4
SLC9A1
Ligand
Receptor
Oligodendrocytes
LAMA2
APP
NEO1
ADAM10
CADM2
ITGA9
GPC1
RGMB
TSPAN17
TSPAN5
CADM3
Ligand
Receptor
OPCs
BMP8A
DSCAM
VCAN
SEMA5A
NRG2
BMP2
FGF14
INHBA
NLGN1
CADM2
VEGFA
OPCML
CNTN3
SLITRK2
NRXN1
KCNA1
THBS4
ACVR2B
PTPRT
SCN1A
SCN2A
SCN8A
EGFR
PLXNA1
LRRTM2
ACVR2A
TGFBR3
SCN3A
NRXN2
ACVR1B
CADM3
GPC1
NEGR1
APP
PTPRD
VSTM2B
CNTN1
CD47
CNTNAP1
Ligand
Receptor
Receiver
Excitatory Neurons
Inhibitory Neurons
B
APP
FGF14
VCAN
SEMA5A
NRG2
BMP2
NRXN1
TGFB1
APOE
SEMA3D
CDH2
SEMA3A
NRG3
FLRT2
APP
GPC1
SCN8A
LRRTM2
ACVR2A
VSTM2B
SCN1A
EGFR
PLXNA1
LRP8
PLXNA4
CDON
UNC5D
PRLR
LMO1
SMAD7
CCND1
Ligand
Receptor
Target
Sender
Astrocytes
Microglia
OPCs
Oligodendrocytes
C
Overlapping Target Genes
PRLR
LMO1
SMAD7
CCND1
Dataset
Morabito
Lau
Cell Type
Excitatory Neurons
Inhibitory Neurons
Pseudo-bulk Expressio
-1
-0.5
0
0.5
1

Table 1. Signaling mediators of ligand-receptor pairs and their downstream targets across datasets.

L-R Pair	Target Gene	Signal Mediators	Top Mediator(s) Morabito et al., 2021	Top Mediator(s) Lau et al., 2020	Receiver Cell Type (Neurons)
FGF14 - SCN8A	*SMAD7*	N/A	N/A	N/A	Inhibitory
VCAN - EGFR	*SMAD7*	*CD44*, *ESR1*, *GSK3B*, *IRAK1*, *JUN*, *MYC*, *SRC*, *STAT3*, *TLR2*, *LCK*, *PTK2*, *STAT1*, *STAT2*	*ESR1*	*MYC*	Inhibitory
VCAN - EGFR	*CCND1*	*CD44*, *ESR1*, *GSK3B*, *IRAK1*, *JUN*, *MYC*, *SRC*, *STAT3*, *TLR2*, *LCK*, *PTK2*, *STAT1*, *STAT2*	*STAT2*	*MYC*	Inhibitory
TGFB1 - APP	*SMAD7*	*SMAD3*, *TP53*, *GSK3B*, *JUN*, *MYC*, *SP1*	*TP53*	*TP53*	Inhibitory
SEMA3D - PLXNA4	*SMAD7*	*CDK5*, *NRP1*, *PAK2*	*CDK5 - EP300*	*CDK5 - EP300*	Inhibitory
SEMA3D - PLXNA1	*SMAD7*	*AKT1*, *CDK5*, *KDR*, *PAK2*	*KDR - NFKB1*	*AKT1 - TP53*	Inhibitory
CDH2 - CDON	*SMAD7*	*CTNNB1*	*CTNNB1*	*CTNNB1*	Inhibitory
SEMA5A - PLXNA1	*SMAD7*	*CDK5*, *PLXNA3*	N/A	*CDK5 - MYC*	Inhibitory
NRG2 - LRRTM2	*SMAD7*	N/A	N/A	N/A	Inhibitory
SEMA3A - PLXNA1	*SMAD7*	*CDK5*	*CDK5 - MYC*	*CDK5 - TP53*	Inhibitory
BMP2 - ACVR2A	*SMAD7*	*MAP3K7*, *SMAD1*, *SMAD3*	*SMAD3*	*SMAD3*	Inhibitory
NRXN1 - VSTM2B	*LMO1*	*TCOF1*	N/A	*TCOF1*	Excitatory
NRG3 - EGFR	*CCND1*	*ERBB2*, *ESR1*, *SRC*, *STAT3*, *CTNNB1*, *MYC*, *PTEN*, *STAT1*, *CCNB1*, *CCND1*, *IFIT3*, *IRF9*, *NFIL3*	Direct	Direct	Inhibitory
FLRT2 - UNC5D	*CCND1*	*DAPK1*, *RAC1*	*RAC1*	*RAC1*	Inhibitory
APOE - LRP8	*CCND1*	*APP*, *LRP1*, *MAPK8*	*MAPK8 - TFAP2A - TP53*	*LRP1 - TP53*	Inhibitory
APP - GPC1	*PRLR*	*MYC*	*MYC*	N/A	Excitatory
FGF14 - SCN1A	*CCND1*	N/A	N/A	N/A	Inhibitory

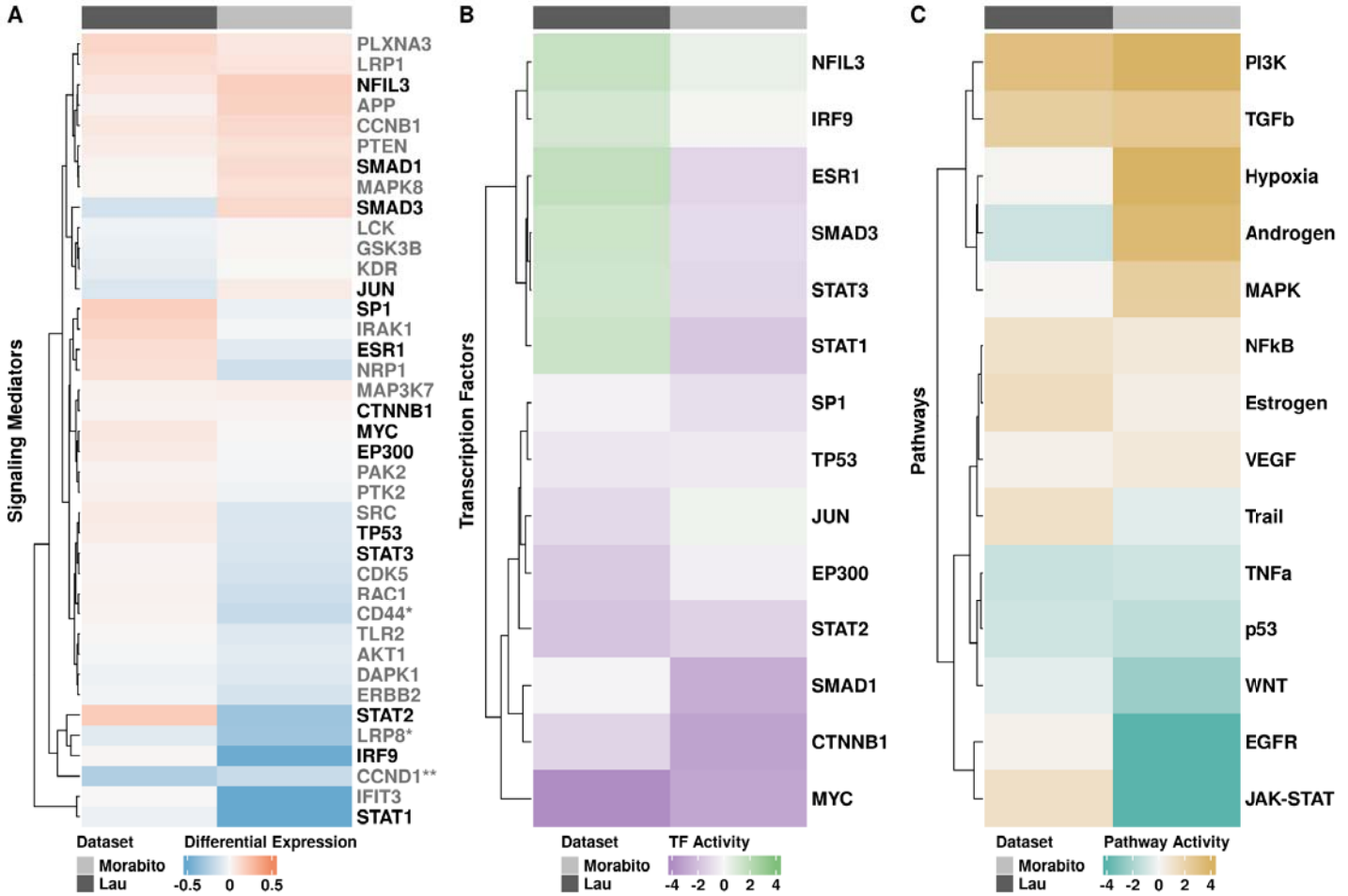

Figure 5. Signaling mediators in inhibitory neurons are not differentially expressed but show altered TF and pathway activity in AD. (A) Heatmap representing pseudo-bulk differential gene expression (DGE) of potential signaling mediators in inhibitory neurons annotated by dataset. Asterisks indicate significant DGE (** in both datasets and * in Morabito et al.). Mediators that are TFs are denoted in black. **(B)** Heatmap of TF activity scores that are different between AD and control of signaling mediators, annotated by dataset. Green and purple represent TF activity as an activator or a repressor, respectively. **(C)** Heatmap of pathway activity scores of all differentially expressed genes in AD from DESeq2 annotated by dataset. Tan and green represent pathway activity as increased or decreased, respectively.

<u>Signaling mediators are not differentially expressed but show altered transcription factor and pathway activity in inhibitory neurons</u>

We constructed gene regulatory networks for all high-confidence interactions using ligand-receptor to target signaling information from MultiNichNet [34] to identify signaling mediators downstream of predicted ligand-receptor pairs. In total, we identified 39 signaling mediators across datasets in inhibitory neurons (**Table 1**). We considered any node adjacent to our receptor node as a potential signaling mediator and predicted the most likely signaling mediators using shortest path calculations with Dijkstra's algorithm between predicted receptors and targets. First, we performed a differential gene expression analysis on pseudo-bulked count data from inhibitory neurons to investigate whether signaling mediators were differentially expressed in AD compared to CTRL. Interestingly, 20 of 39 signaling mediators had divergent gene expression across our datasets, and we observed that only *CCND1* was significantly downregulated in both (**Fig 5A**). Additionally, two genes were significantly different in AD in the Morabito et al. data (*LRP8* and *CD44*; p-value < 0.05), however, neither *LRP8* nor *CD44* was significant in the Lau et al. data. Since most of our predicted signaling

mediators were not differentially expressed in AD, this could indicate that their downstream effects may be due to gene regulatory mechanisms instead of gene expression, therefore, we investigated their TF activity. Using pseudo-bulked gene expression information from inhibitory neurons, we calculated TF activity scores for 14 signaling mediators that were also TFs. While none of the TFs were differentially expressed, 8 out of 14 had divergent gene expression patterns across datasets (gene expression was increased in only one dataset and vice versa, **Fig 5A**). Overall, MYC, CTNNB1, SMAD1, STAT2, EP300, TP53, and SP1 consistently function as repressors, suggesting that they downregulate their target genes in AD inhibitory neurons across datasets (**Fig 5B**). MYC, a cancer-associated cell cycle regulator [56], showed the greatest overall significant difference in TF activity in AD (**Fig 5B**). *MYC* had slightly increased expression (logfc of 0.008 and 0.073 in Morabito and Lau, respectively; **Fig 5A**) while downregulating its targets in AD (**Fig 5B**). Additionally, CTNNB1, which is associated with cell-cell adhesion regulation and coordination [57], also significantly downregulates its targets in AD in the Morabito et al. dataset (**Fig 5B**). Like *MYC*, *CTNNB1* also had increased expression in AD (logfc of 0.021 and 0.026 in Morabito and Lau, respectively; **Fig 5A**). Both *CTNNB1* and *MYC* are involved in the WNT signaling pathway [58], which was decreased in AD (**Fig 5C**). Interestingly, despite their divergent gene expression patterns (downregulated in Morabito, upregulated in Lau; **Fig 5A**), TP53 and its transcriptional cofactor EP300 [59] function as transcriptional repressors in AD (**Fig 5B**), which is further recapitulated by decreased p53 signaling pathway activity in inhibitory neurons (**Fig 5C**). NFIL3 and IRF9, associated with NF-kappaB (NFkB) [60] and type I interferon signaling [61], respectively, were the only TFs to function as transcriptional activators across both datasets in AD (**Fig 5B**). Along with high TF activity, we observed increased *NFIL3* expression (**Fig 5A**) and high activity of the NFkB signaling pathway (**Fig 5C**) in AD, which were both consistent across datasets. The expression of *IRF9* was not consistent across datasets (increased in Lau et al. and decreased in Morabito et al., **Fig 5A**) in AD, and we were unable to predict type I interferon signaling activity. All other TFs, including STAT1, STAT3, SMAD3, ESR1, and JUN showed divergent TF activity across datasets. STAT1, STAT3, SMAD3, and ESR1 activity was increased in Lau et al. and decreased in Morabito et al., while JUN activity was reversed (**Fig 5B**). Interestingly, there was STAT2 repressor activity in both datasets in AD, while STAT1 and STAT3 TF activities were different across datasets (**Fig 5B**); therefore it was not surprising that JAK-STAT signaling in AD was decreased in Morabito et al. and increased in Lau et al. (**Fig 5C**). Overall, we find consistently altered TF and pathway activity associated with WNT, p53, and NFkB signaling dysregulation in inhibitory neurons across datasets despite the lack of significant gene expression changes of signaling mediators. This further suggests gene regulatory consequences of altered CCC between glia and neurons in AD.

Discussion

In this study, we investigated altered CCC in two publicly available snRNA-seq datasets from postmortem human PFC in AD using *in silico* approaches to generate high-confidence LRT interactions. Previous *in silico* studies have either investigated overall CCC patterns across all brain cell types without specifically describing glia-neuron interactions and their downstream effects or focused on interactions between excitatory neurons and microglia [29–31]. Here, we predicted interactions between glia (astrocytes, microglia, oligodendrocytes, and OPCs) and neurons (excitatory and inhibitory), while also investigating their potential downstream consequences in inhibitory neurons. Although neuronal loss is a primary hallmark of AD, glia are important for maintaining brain homeostasis and neuronal health through interactions with neuronal cell populations [3–6]. For example, astrocytes provide metabolic and nutritional support [7, 8], oligodendrocytes myelinate neuronal axons [9], microglia respond to injury affecting neuronal function [11–13], and OPCs make direct contact with neuronal synapses [10]. Consistent with previous studies [29, 30], our JI analyses of ligands, receptors, and targets confirm that interactions between glia and neurons are altered in a cell-type-specific manner in AD. Although ligands are known to target many receptors across different cells, causing a variety of downstream effects [62, 63], a previous study in hematopoietic stem cells revealed greater cell-type-specificity in ligands than receptors [64]. Our findings corroborate this in the PFC, as we observed the greatest cell-type-specificity

in ligands, followed by receptors and then targets. Finally, since our high-confidence interactions converge to 4 downstream target genes, it is plausible that although ligand-receptor pairs are sender-specific, the aggregated effects of altered glia-neuron communication converge in both excitatory and inhibitory neurons.

Our high-confidence interactions included *APP*, a familial AD risk gene, and *APOE*, the strongest genetic risk factor of sporadic AD [65], which has previously been confirmed as a ligand for another AD-risk gene, *TREM2*. A recent study has shown the involvement of APOE as a ligand in astrocyte-neuron interactions through the receptors LRP1 and SORL1 in both inhibitory and excitatory neurons [31]. Interestingly, we predicted an interaction of APOE with a different low-density lipoprotein receptor, LRP8, between astrocytes and inhibitory neurons. Even though the association of LRP8 with AD was not robust in previous work [66], the APOE-LRP8 interaction was among our high-confidence interactions. Additionally, low-density lipoprotein receptors have high and isoform-specific binding affinity for *APOE* [67]. Combined, this suggests a potential role for receptors in the low-density lipoprotein receptor family in AD that requires further investigation.

Additionally, semaphorins are signaling proteins that most often bind to plexin receptors crucial to neurodevelopment and the adult CNS [68]. Immunohistochemistry work in the human brain illustrated that semaphorin3A (SEMA3A) colocalizes with tau neurofibrillary tangles in neurons during the later stages of AD [69]. SEMA3A has also been indicated to induce activation of cyclin-dependent kinase 5 (CDK5), promoting phosphorylation of tau neurofibrillary tangles [69, 70]. Our data further support these initial findings, as we predicted 4 high-confidence interactions involving semaphorin ligands and plexin receptors. Interestingly, we also showed the involvement of *CDK5* as a signaling mediator for 3 of the 4 predicted semaphorin-plexin interactions. Additionally, SEMA6D interacts with TREM2 through altered neuron-microglia interactions, regulating microglia activation in AD [30]. This further indicates the importance of semaphorins in AD, as their signaling is altered between multiple sender and receiver cell types across patient cohorts.

Canonical signaling through the WNT [15, 16], p53 [24], and NFkB [22, 23] signaling pathways have been shown to be dysregulated in AD. The WNT signaling pathway is crucial for normal brain function and neuronal survival in the adult CNS and has been extensively implicated in AD (reviewed in [15, 16]). Interestingly, our pathway activity analyses indicated decreased WNT signaling in AD inhibitory neurons. Increased levels of Wnt signaling have been shown to have a protective role against amyloid-β plaques in both *in vitro* and *in vivo* models of AD [71–73]. We also identified *MYC* and *CTNNB1* as potential signaling mediators of high-confidence interactions in inhibitory neurons. *MYC* is at the crossroads of multiple signaling pathways, including WNT signaling [58], and its increased expression leads to elevated vulnerability of neurons in degenerative diseases [74]. *CTNNB1* is a key player in the WNT signaling pathway [57]. In concordance with the literature, we observed increased expression of *MYC* and *CTNNB1*, increased repressor TF activity for both, and overall decreased WNT signaling in AD. Furthermore, the p53 signaling pathway is often associated with carcinogenesis due to its role in DNA damage and cellular stress responses, but there is mounting evidence of its involvement in AD. *In vitro* data indicates increased levels of p53 expression [75], which we also observed. Additionally, the inactivation of the p53 pathway is known to lead to cell cycle re-entry of senescent cells [76], and, in AD, neuronal cell cycle re-entry exacerbates neuronal loss [77, 78]. While we found different gene expression patterns of *TP53* and its co-regulator *EP300* across datasets, we identified repressor TF activity of TP53 and EP300 and decreased p53 signaling pathway activity in AD inhibitory neurons consistent across datasets. The NFkB signaling pathway regulates the expression of proinflammatory genes in the context of immunity [79]. It has also been shown to be associated with neuroinflammation in AD (reviewed in [22, 23]), as well as amyloid-β plaque and tau neurofibrillary tangle pathologies (reviewed in [80]). Multiple studies have shown that amyloid-β accumulation in AD leads to neurotoxic activation of the NFkB signaling pathway [80], which may lead to activation of Beta-site APP cleaving enzyme 1 (BACE1), initiating the formation of amyloid-beta through splicing of *APP* [81]. Interestingly, we observed differential *NFIL3* gene

expression between AD and CTRL and activator TF activity in AD of NFIL3, an important regulator of the NFkB signaling pathway, consistent across datasets. We also observed increased activity of the NFkB signaling pathway in inhibitory neurons in AD. Altogether, this suggests that altered glia-neuron interactions may play a role in dysregulating canonical signaling pathways like WNT, p53, and NFkB signaling in inhibitory neurons in AD.

Although our study provides insight into dysregulated glia-neuron interactions and their downstream effects in AD, there are limitations including the use of curated priors for CCC and biological activity inference and postmortem data with varying sequencing depth and number of nuclei. Our CCC inference relies on curated priors, therefore, any interactions that have not been described previously are excluded from the prior, limiting our ability to predict entirely novel interactions. Additionally, we inferred protein abundances of ligands and receptors from gene expression information. Due to multiple processes like post-translational modifications and protein degradation, mRNA and protein levels are not always directly related. Therefore, our hypothesis-generating approach calls for further confirmation of predicted interaction through additional experimentation (e.g.,RNAscope or co-culture) in future studies with access to appropriate samples. Similarly, TF and pathway activity analyses also rely on previously curated priors. Finally, despite our best efforts to choose comparable datasets, there was extensive technical variability between datasets (number of nuclei and sequencing depth). While AD is a heterogeneous and multifactorial disorder, we expected greater LRT overlap. This suggests that the technical variability between the two snRNA-seq datasets in our study might be a confounding factor. As more snRNA-seq datasets with increased sequencing depth and number of nuclei become available, our analyses should be expanded to confirm and extend findings from the present study. Finally, we are using data generated from postmortem human brains, a timepoint where extensive neuronal degeneration and loss has occurred. Therefore, we are likely not capturing the altered CCC patterns relevant to disease etiology and progression. Future studies should investigate altered signaling across time points or disease stages (e.g., in AD mouse models) to properly address how disease progression affects CCC in AD.

Conclusions

Overall, using public snRNA-seq data from postmortem human PFC, we inferred altered cell-type-specific CCC between glia and neurons in AD. We find that the AD-risk genes *APP* and *APOE* are among altered interactions conserved across patient cohorts. Additionally, we observed altered TF activity of signaling mediators, along with altered signaling pathway activity, in inhibitory neurons. Therefore, our findings suggest that altered glia-neuron interactions may dysregulate canonical signaling in pathways like WNT, p53, and NFkB through TFs and co-regulators like MYC, CTNNB1, TP53, EP300, and NFIL3.

Abbreviations

AD	Alzheimer’s disease
OPC	oligodendrocyte progenitor cell
CNS	central nervous system
CCC	cell-cell communication
snRNA-seq	single-nucleus RNA sequencing
PFC	prefrontal cortex
JI	Jaccard Similarity Index
TF	transcription factor
CTRL	control
PCA	Principal Component Analysis
UMAP	Uniform Manifold Approximation and Projection
LRT	ligand-receptor-target
DGE	differential gene expression

SEMA3A	semaphorin3A
CDK5	cyclin-dependent kinase 5

Declarations

Ethics approval and consent to participate

Not applicable

Consent for publication

Not applicable

Availability of data and materials

The snRNA-sequencing datasets used in this study were downloaded from the GEO database (GSE174367 [32], GSE157827 [33]). The data of this study are available on Zenodo (doi: 10.5281/zenodo.10214497). The code supporting the results of this study is available on Zenodo (doi: 10.5281/zenodo.10211622) and https://github.com/lasseignelab/230313_TS_CCCinHumanAD. Docker images used for these analyses are publicly available on Docker Hub (https://hub.docker.com/repository/docker/tsoelter/rstudio_ccc_ad/general) and Zenodo (doi: 10.5281/zenodo.10214660).

Competing interests

The authors declare that they do not have competing interests.

Funding

This work was supported in part by the UAB Lasseigne Lab funds (to BNL; supported TMS, TCH, ADC, VHO), R00HG009678-04S1 (to BNL; also supported TMS), TMS was funded by the Alzheimer's of Central Alabama Lindy Harrell Predoctoral Scholar Program.

Authors' contributions

TMS, VHO, TCH, and BNL conceptualized the project. TMS downloaded and performed preprocessing. TMS adapted code from VHO for Jaccard Similarity Index calculations. All other analyses were coded and performed by TMS. TCH, ADC, and VHO reviewed and validated the code. BNL provided supervision and project administration. BNL and TMS acquired funding. TMS wrote the first draft. TMS, TCH, ADC, VHO, and BNL reviewed and edited the manuscript. All authors read and approved the final manuscript.

Acknowledgments

The authors thank the Lasseigne Lab members Jordan Whitlock, Emma Jones, and Elizabeth Wilk for their feedback throughout this study. We also thank the UAB Biological Data Science group (RRID:SCR_021766) for providing a script for helping to run containers on the UAB high-performance cluster (https://github.com/U-BDS/training_guides/blob/main/run_rstudio_singularity.sh).

References

1. Emmady PD, Schoo C, Tadi P (2022) Major Neurocognitive Disorder (Dementia). StatPearls Publishing

2. What causes Alzheimer's disease? In: National Institute on Aging. https://www.nia.nih.gov/health/what-causes-alzheimers-disease. Accessed 30 Aug 2023

3. Matejuk A, Ransohoff RM (2020) Crosstalk Between Astrocytes and Microglia: An Overview. Front Immunol. https://doi.org/10.3389/fimmu.2020.01416

4. Pan J, Ma N, Yu B, Zhang W, Wan J (2020) Transcriptomic profiling of microglia and astrocytes throughout aging. J Neuroinflammation 17:1–19

5. Sheridan GK, Murphy KJ (2013) Neuron-glia crosstalk in health and disease: fractalkine and CX3CR1 take centre stage. Open Biol 3:130181

6. Bernaus A, Blanco S, Sevilla A (2020) Glia Crosstalk in Neuroinflammatory Diseases. Front Cell Neurosci 14:209

7. Turner DA, Adamson DC (2011) Neuronal-astrocyte metabolic interactions: understanding the transition into abnormal astrocytoma metabolism. J Neuropathol Exp Neurol 70:167–176

8. Santello M, Toni N, Volterra A (2019) Astrocyte function from information processing to cognition and cognitive impairment. Nat Neurosci 22:154–166

9. Bradl M, Lassmann H (2010) Oligodendrocytes: biology and pathology. Acta Neuropathol 119:37–53

10. Fang L-P, Bai X (2023) Oligodendrocyte precursor cells: the multitaskers in the brain. Pflugers Arch 475:1035–1044

11. Clayton KA, Van Enoo AA, Ikezu T (2017) Alzheimer's Disease: The Role of Microglia in Brain Homeostasis and Proteopathy. Front Neurosci 11:680

12. Szepesi Z, Manouchehrian O, Bachiller S, Deierborg T (2018) Bidirectional Microglia-Neuron Communication in Health and Disease. Front Cell Neurosci 12:323

13. Augusto-Oliveira M, Arrifano GP, Lopes-Araújo A, Santos-Sacramento L, Takeda PY, Anthony DC, Malva JO, Crespo-Lopez ME (2019) What Do Microglia Really Do in Healthy Adult Brain? Cells. https://doi.org/10.3390/cells8101293

14. Cummings J, Lee G, Ritter A, Sabbagh M, Zhong K (2019) Alzheimer's disease drug development pipeline: 2019. Alzheimers Dement 5:272–293

15. Aghaizu ND, Jin H, Whiting PJ (2020) Dysregulated Wnt Signalling in the Alzheimer's Brain. Brain Sci. https://doi.org/10.3390/brainsci10120902

16. Palomer E, Buechler J, Salinas PC (2019) Wnt Signaling Deregulation in the Aging and Alzheimer's Brain. Front Cell Neurosci 13:227

17. von Bernhardi R, Cornejo F, Parada GE, Eugenín J (2015) Role of TGFβ signaling in the pathogenesis of Alzheimer's disease. Front Cell Neurosci 9:426

18. Das P, Golde T (2006) Dysfunction of TGF-beta signaling in Alzheimer's disease. J Clin Invest 116:2855–2857

19. Kapoor M, Chinnathambi S (2023) TGF-β1 signalling in Alzheimer's pathology and cytoskeletal reorganization: a specialized Tau perspective. J Neuroinflammation 20:72

20. Perluigi M, Di Domenico F, Barone E, Butterfield DA (2021) mTOR in Alzheimer disease and its earlier stages: Links to oxidative damage in the progression of this dementing disorder. Free Radic Biol Med 169:382–396

21. Oddo S (2012) The role of mTOR signaling in Alzheimer disease. Front Biosci 4:941–952

22. Sun E, Motolani A, Campos L, Lu T (2022) The Pivotal Role of NF-kB in the Pathogenesis and Therapeutics of Alzheimer's Disease. Int J Mol Sci. https://doi.org/10.3390/ijms23168972

23. Ju Hwang C, Choi D-Y, Park MH, Hong JT (2019) NF-κB as a Key Mediator of Brain Inflammation in

Alzheimer's Disease. CNS Neurol Disord Drug Targets 18:3–10

24. Wolfrum P, Fietz A, Schnichels S, Hurst J (2022) The function of p53 and its role in Alzheimer's and Parkinson's disease compared to age-related macular degeneration. Front Neurosci 16:1029473

25. Razani E, Pourbagheri-Sigaroodi A, Safaroghli-Azar A, Zoghi A, Shanaki-Bavarsad M, Bashash D (2021) The PI3K/Akt signaling axis in Alzheimer's disease: a valuable target to stimulate or suppress? Cell Stress Chaperones 26:871–887

26. Kumar M, Bansal N (2022) Implications of Phosphoinositide 3-Kinase-Akt (PI3K-Akt) Pathway in the Pathogenesis of Alzheimer's Disease. Mol Neurobiol 59:354–385

27. Yu H-J, Koh S-H (2017) The role of PI3K/AKT pathway and its therapeutic possibility in Alzheimer's disease. Hanyang Med Rev 37:18–24

28. Almet AA, Cang Z, Jin S, Nie Q (2021) The landscape of cell-cell communication through single-cell transcriptomics. Curr Opin Syst Biol 26:12–23

29. Lee CY, Riffle D, Xiong Y, Momtaz N, Hwang A, Duan Z, Zhang J (2023) Characterizing dysregulations via cell-cell communications in Alzheimer's brains using single-cell transcriptomes. bioRxiv 2023.07.16.548274

30. Albanus RD, Finan GM, Brase L, et al (2023) Systematic analysis of cellular crosstalk reveals a role for SEMA6D-TREM2 regulating microglial function in Alzheimer's disease. bioRxiv 2022.11.11.516215

31. Liu A, Fernandes BS, Citu C, Zhao Z (2023) Unraveling the intercellular communication disruption and key pathways in Alzheimer's disease: An integrative study of single-nucleus transcriptomes and genetic association. Res Sq. https://doi.org/10.21203/rs.3.rs-3335643/v1

32. Morabito S, Miyoshi E, Michael N, Shahin S, Martini AC, Head E, Silva J, Leavy K, Perez-Rosendahl M, Swarup V (2021) Single-nucleus chromatin accessibility and transcriptomic characterization of Alzheimer's disease. Nat Genet 53:1143–1155

33. Lau S-F, Cao H, Fu AKY, Ip NY (2020) Single-nucleus transcriptome analysis reveals dysregulation of angiogenic endothelial cells and neuroprotective glia in Alzheimer's disease. Proc Natl Acad Sci U S A 117:25800

34. Browaeys R, Gilis J, Sang-Aram C, De Bleser P, Hoste L, Tavernier S, Lambrechts D, Seurinck R, Saeys Y (2023) MultiNicheNet: a flexible framework for differential cell-cell communication analysis from multi-sample multi-condition single-cell transcriptomics data. bioRxiv 2023.06.13.544751

35. Badia-I-Mompel P, Vélez Santiago J, Braunger J, et al (2022) decoupleR: ensemble of computational methods to infer biological activities from omics data. Bioinform Adv 2:vbac016

36. Zheng GXY, Terry JM, Belgrader P, et al (2017) Massively parallel digital transcriptional profiling of single cells. Nat Commun 8:14049

37. Merkel D Docker: lightweight Linux containers for consistent development and deployment. Linux J.

38. Young MD, Behjati S (2020) SoupX removes ambient RNA contamination from droplet-based single-cell RNA sequencing data. Gigascience. https://doi.org/10.1093/gigascience/giaa151

39. Satija R, Farrell JA, Gennert D, Schier AF, Regev A (2015) Spatial reconstruction of single-cell gene expression data. Nat Biotechnol 33:495–502

40. Korsunsky I, Fan J, Slowikowski K, Zhang F, Wei K, Baglaenko Y, Brenner M, Loh P-R, Raychaudhuri S (2018) Fast, sensitive, and accurate integration of single cell data with Harmony. bioRxiv 461954

41. Luecken MD, Büttner M, Chaichoompu K, et al (2022) Benchmarking atlas-level data integration in single-cell genomics. Nat Methods 19:41–50

42. Zappia L, Oshlack A (2018) Clustering trees: a visualization for evaluating clusterings at multiple resolutions. Gigascience. https://doi.org/10.1093/gigascience/giy083

43. Traag VA, Waltman L, van Eck NJ (2019) From Louvain to Leiden: guaranteeing well-connected communities. Sci Rep 9:5233

44. Franzén O, Gan L-M, Björkegren JLM (2019) PanglaoDB: a web server for exploration of mouse and human single-cell RNA sequencing data. Database . https://doi.org/10.1093/database/baz046

45. Zhang X, Lan Y, Xu J, et al (2019) CellMarker: a manually curated resource of cell markers in human and mouse. Nucleic Acids Res 47:D721–D728

46. Karlsson M, Zhang C, Méar L, et al (2021) A single-cell type transcriptomics map of human tissues. Sci Adv. https://doi.org/10.1126/sciadv.abh2169

47. Amezquita RA, Lun ATL, Becht E, et al (2020) Orchestrating single-cell analysis with Bioconductor. Nat Methods 17:137–145

48. Csárdi G, Nepusz T, Müller K, Horvát S, Traag V, Zanini F, Noom D (2023) igraph for R: R interface of the igraph library for graph theory and network analysis. https://doi.org/10.5281/ZENODO.7682609

49. Luecken MD, Theis FJ (2019) Current best practices in single-cell RNA-seq analysis: a tutorial. Mol Syst Biol 15:e8746

50. Whitlock JH, Soelter TM, Howton TC, Wilk EJ, Oza VH, Lasseigne BN (2023) Cell-type-specific gene expression and regulation in the cerebral cortex and kidney of atypical Setbp1S858R Schinzel Giedion Syndrome mice. J Cell Mol Med 27:3565–3577

51. Love MI, Huber W, Anders S (2014) Moderated estimation of fold change and dispersion for RNA-seq data with DESeq2. Genome Biol 15:550

52. Müller-Dott S, Tsirvouli E, Vázquez M, Ramirez Flores RO, Badia-i-Mompel P, Fallegger R, Lægreid A, Saez-Rodriguez J (2023) Expanding the coverage of regulons from high-confidence prior knowledge for accurate estimation of transcription factor activities. bioRxiv 2023.03.30.534849

53. Schubert M, Klinger B, Klünemann M, Sieber A, Uhlitz F, Sauer S, Garnett MJ, Blüthgen N, Saez-Rodriguez J (2018) Perturbation-response genes reveal signaling footprints in cancer gene expression. Nat Commun 9:20

54. Wang L, Chiang H-C, Wu W, Liang B, Xie Z, Yao X, Ma W, Du S, Zhong Y (2012) Epidermal growth factor receptor is a preferred target for treating amyloid-β-induced memory loss. Proc Natl Acad Sci U S A 109:16743–16748

55. Choi H-J, Jeong YJ, Kim J, Hoe H-S (2023) EGFR is a potential dual molecular target for cancer and Alzheimer's disease. Front Pharmacol 14:1238639

56. Ahmadi SE, Rahimi S, Zarandi B, Chegeni R, Safa M (2021) MYC: a multipurpose oncogene with prognostic and therapeutic implications in blood malignancies. J Hematol Oncol 14:121

57. Zhuang W, Ye T, Wang W, Song W, Tan T (2023) CTNNB1 in neurodevelopmental disorders. Front Psychiatry 14:1143328

58. Jahangiri L, Pucci P, Ishola T, Trigg RM, Williams JA, Pereira J, Cavanagh ML, Turner SD, Gkoutos GV, Tsaprouni L (2021) The Contribution of Autophagy and LncRNAs to MYC-Driven Gene Regulatory

Networks in Cancers. Int J Mol Sci. https://doi.org/10.3390/ijms22168527

59. Grossman SR (2001) p300/CBP/p53 interaction and regulation of the p53 response. Eur J Biochem 268:2773–2778

60. Zhuo H, Liu J (2022) Nuclear factor interleukin 3 (NFIL3) participates in regulation of the NF-κB-mediated inflammation and antioxidant system in Litopenaeus vannamei under ammonia-N stress. Fish Shellfish Immunol 131:1192–1205

61. Paul A, Tang TH, Ng SK (2018) Interferon Regulatory Factor 9 Structure and Regulation. Front Immunol 9:1831

62. Heldin C-H, Lu B, Evans R, Gutkind JS (2016) Signals and Receptors. Cold Spring Harb Perspect Biol 8:a005900

63. Miller EJ, Lappin SL (2022) Physiology, Cellular Receptor. StatPearls Publishing

64. Qiao W, Wang W, Laurenti E, Turinsky AL, Wodak SJ, Bader GD, Dick JE, Zandstra PW (2014) Intercellular network structure and regulatory motifs in the human hematopoietic system. Mol Syst Biol 10:741

65. Strittmatter WJ, Saunders AM, Schmechel D, Pericak-Vance M, Enghild J, Salvesen GS, Roses AD (1993) Apolipoprotein E: high-avidity binding to beta-amyloid and increased frequency of type 4 allele in late-onset familial Alzheimer disease. Proc Natl Acad Sci U S A 90:1977–1981

66. Ma SL, Ng HK, Baum L, Pang JCS, Chiu HFK, Woo J, Tang NLS, Lam LCW (2002) Low-density lipoprotein receptor-related protein 8 (apolipoprotein E receptor 2) gene polymorphisms in Alzheimer's disease. Neurosci Lett 332:216–218

67. Johnson LA, Olsen RHJ, Merkens LS, DeBarber A, Steiner RD, Sullivan PM, Maeda N, Raber J (2014) Apolipoprotein E-low density lipoprotein receptor interaction affects spatial memory retention and brain ApoE levels in an isoform-dependent manner. Neurobiol Dis 64:150–162

68. Alto LT, Terman JR (2017) Semaphorins and their Signaling Mechanisms. Methods Mol Biol 1493:1–25

69. Good PF, Alapat D, Hsu A, Chu C, Perl D, Wen X, Burstein DE, Kohtz DS (2004) A role for semaphorin 3A signaling in the degeneration of hippocampal neurons during Alzheimer's disease. J Neurochem 91:716–736

70. Uchida Y, Ohshima T, Sasaki Y, et al (2005) Semaphorin3A signalling is mediated via sequential Cdk5 and GSK3beta phosphorylation of CRMP2: implication of common phosphorylating mechanism underlying axon guidance and Alzheimer's disease. Genes Cells 10:165–179

71. De Ferrari GV, Chacón MA, Barría MI, Garrido JL, Godoy JA, Olivares G, Reyes AE, Alvarez A, Bronfman M, Inestrosa NC (2003) Activation of Wnt signaling rescues neurodegeneration and behavioral impairments induced by beta-amyloid fibrils. Mol Psychiatry 8:195–208

72. Alvarez AR, Godoy JA, Mullendorff K, Olivares GH, Bronfman M, Inestrosa NC (2004) Wnt-3a overcomes beta-amyloid toxicity in rat hippocampal neurons. Exp Cell Res 297:186–196

73. Chacón MA, Varela-Nallar L, Inestrosa NC (2008) Frizzled-1 is involved in the neuroprotective effect of Wnt3a against Abeta oligomers. J Cell Physiol 217:215–227

74. Marinkovic T, Marinkovic D (2021) Obscure Involvement of MYC in Neurodegenerative Diseases and Neuronal Repair. Mol Neurobiol 58:4169–4177

75. Hooper C, Meimaridou E, Tavassoli M, Melino G, Lovestone S, Killick R (2007) p53 is upregulated in

Alzheimer's disease and induces tau phosphorylation in HEK293a cells. Neurosci Lett 418:34–37

76. Beauséjour CM, Krtolica A, Galimi F, Narita M, Lowe SW, Yaswen P, Campisi J (2003) Reversal of human cellular senescence: roles of the p53 and p16 pathways. EMBO J 22:4212–4222

77. Koseoglu MM, Norambuena A, Sharlow ER, Lazo JS, Bloom GS (2019) Aberrant Neuronal Cell Cycle Re-Entry: The Pathological Confluence of Alzheimer's Disease and Brain Insulin Resistance, and Its Relation to Cancer. J Alzheimers Dis 67:1–11

78. Farmer KM, Ghag G, Puangmalai N, Montalbano M, Bhatt N, Kayed R (2020) P53 aggregation, interactions with tau, and impaired DNA damage response in Alzheimer's disease. Acta Neuropathol Commun 8:132

79. Yu H, Lin L, Zhang Z, Zhang H, Hu H (2020) Targeting NF-κB pathway for the therapy of diseases: mechanism and clinical study. Signal Transduct Target Ther 5:209

80. Snow WM, Albensi BC (2016) Neuronal Gene Targets of NF-κB and Their Dysregulation in Alzheimer's Disease. Front Mol Neurosci 9:118

81. Cole SL, Vassar R (2007) The Alzheimer's disease beta-secretase enzyme, BACE1. Mol Neurodegener 2:22